Observation of VHE γ-rays from Cassiopeia A with the MAGIC telescope

J. Albert[1], E. Aliu[2], H. Anderhub[3], P. Antoranz[4], A. Armada[2], C. Baixeras[5], J. A. Barrio[4] H. Bartko[6], D. Bastieri[7], J. K. Becker[8], W. Bednarek[9], K. Berger[1], C. Bigongiari[7], A. Biland[3], R. K. Bock[6,7], P. Bordas[10], V. Bosch-Ramon[10], T. Bretz[1], I. Britvitch[3], M. Camara[4], E. Carmona[6], A. Chilingarian[11], J. A. Coarasa[6], S. Commichau[3], J. L. Contreras[4], J. Cortina[2], M.T. Costado[13], V. Curtef[8], V. Danielyan[11], F. Dazzi[7], A. De Angelis[14], C. Delgado[13], R. de los Reyes[4], B. De Lotto[14], E. Domingo-Santamaría[2], D. Dorner[1], M. Doro[7], M. Errando[2], M. Fagiolini[15], D. Ferenc[16], E. Fernández[2], R. Firpo[2], J. Flix[2], M. V. Fonseca[4], L. Font[5], M. Fuchs[6], N. Galante[6], R. García-López[13], M. Garczarczyk[6], M. Gaug[13], M. Giller[9], F. Goebel[6], D. Hakobyan[11], M. Hayashida[6], T. Hengstebeck[17], A. Herrero[13], D. Höhne[1], J. Hose[6], C. C. Hsu[6], P. Jacon[9], T. Jogler[6], R. Kosyra[6], D. Kranich[3], R. Kritzer[1], A. Laille[16], E. Lindfors[12], S. Lombardi[7], F. Longo[14], J. López[2], M. López[4], E. Lorenz[3,6], P. Majumdar[6], G. Maneva[18], K. Mannheim[1], O. Mansutti[14], M. Mariotti[7], M. Martínez[2], D. Mazin[6], C. Merck[6], M. Meucci[15], M. Meyer[1], J. M. Miranda[4], R. Mirzoyan[6], S. Mizobuchi[6], A. Moralejo[2], K. Nilsson[12], J. Ninkovic[6], E. Oña-Wilhelmi[2*], N. Otte[6], I. Oya[4], D. Paneque[6], M. Panniello[13], R. Paoletti[15], J. M. Paredes[10], M. Pasanen[12], D. Pascoli[7], F. Pauss[3], R. Pegna[15], M. Persic[14,19], L. Peruzzo[7], A. Piccioli[15], M. Poller[1], N. Puchades[2], E. Prandini[7], A. Raymers[11], W. Rhode[8], M. Ribó[10], J. Rico[2], M. Rissi[3], A. Robert[5], S. Rügamer[1], A. Saggion[7], A. Sánchez[5], P. Sartori[7], V. Scalzotto[7], V. Scapin[14], R. Schmitt[1], T. Schweizer[6], M. Shayduk[17,6], K. Shinozaki[6], S. N. Shore[20], N. Sidro[2], A. Sillanpää[12], D. Sobczynska[9], A. Stamerra[15], L. S. Stark[3], L. Takalo[12], P. Temnikov[18], D. Tescaro[2], M. Teshima[6], N. Tonello[6], D. F. Torres[21], N. Turini[15], H. Vankov[18], V. Vitale[14], R. M. Wagner[6], T. Wibig[9], W. Wittek[6], F. Zandanel[7], R. Zanin[2], and J. Zapatero[5]

(Affiliations can be found after the references)

ABSTRACT

Aims. We searched for very high energy (VHE) γ-ray emission from the supernova remnant Cassiopeia A

Methods. The shell-type supernova remnant Cassiopeia A was observed with the 17 meter MAGIC telescope between July 2006 and January 2007 for a total time of 47 hours.

Results. The source was detected above an energy of 250 GeV with a significance of 5.2 σ and a photon flux above 1 TeV of $(7.3\pm0.7_{stat}\pm2.2_{sys})\times 10^{-13} cm^{-2} s^{-1}$. The photon spectrum is compatible with a power law $dN/dE \propto E^{-\Gamma}$ with a photon index $\Gamma=2.3\pm0.2_{stat}\pm0.2_{sys}$. The source is point-like within the angular resolution of the telescope.

Key words. acceleration of particles - ISM: cosmic rays - gamma rays: observations - ISM: supernova remnants - gamma rays: individual objects: Cassiopeia A

1. Introduction

Cassiopeia A (Cas A), with right ascension (RA) and declination (DEC) $(23.385^h, 58.800^o)$, is a prominent shell type supernova remnant and a bright source of synchrotron radiation observed at radio frequencies, see Bell et al. (1975); Tuffs et al. (1986), and in the X-ray band, see Allen et al. (1997), Favata et al. (1997). The remnant results from the youngest known Galactic supernova, whose explosion took place around 1680. Its distance was estimated at 3.4 kpc by Reed et al. (1995). High resolution X-ray images from the Chandra satellite, see Hughes et al. (2000), reveal a shell-type nature of the remnant and the existence of a central object. The progenitor of Cas A was probably a Wolf-Rayet star, as discussed in Fesen et al. (1991) and Iyudin et al.

(1997). The progenitor's initial mass was large, estimated to be between 15 and 25 $M_\odot$, see Young et al. (2006). The morphology of the remnant as seen in optical, X-ray and IR wavelength consists on a patchy and irregular shell with a diameter of 4' (4 pc at 3.4 kpc). The supernova blast wave is expanding into a wind bubble formed from the previous wind phases of the progenitor star; this plays an important role in shock acceleration of CR, see Berezhko et al. (2003).

At TeV energies, Cas A was detected by the HEGRA Stereoscopic Cherenkov Telescope System, which accumulated 232 hours of data from 1997 to 1999. TeV γ-ray emission was detected at 5σ level and a flux of $(5.8 \pm 1.2_{stat}\pm1.2_{sys}) 10^{-13}$ ph cm^{-2}s^{-1} above 1 TeV was derived, as discussed in Aharonian et al. (2001). The spectral distribution between 1 and 10 TeV was found to be consistent with a power law with a differential spectral index of $-2.5\pm0.4_{stat}\pm0.1_{sys}$. Upper limits at TeV energies have been set also by Whipple, see Lessard et al. (1999) and CAT, see Goret et al. (1999). These up-

per limits were consistent with the HEGRA detected flux level. At lower energy, EGRET set an upper limit for a flux below 12.4×10^{-8} cm^{-2}s^{-1}, see Esposito et al. (1996).

The HEGRA detection makes Cas A a good scenario to test the supernova remnant emission at lower energies, in particular for trying to further distinguish between leptonic and hadronic models for the origin of the γ-ray emission. A summary of the observations and analysis results is given in Section 2, the results are reported in Section 3 and finally a comparison of MAGIC detection with the existing model predictions for the TeV γ-ray emission on Cas A is discussed in Section 4.

2. Observations and Data Analysis

The MAGIC (Major Atmospheric Gamma Imaging Cherenkov) Telescope is located on the Canary Island La Palma (2200 m asl, $28°45'N$, $17°54'W$) and has a 17 m-diameter tessellated reflector dish, see Cortina et al. (2005). The total field of view is $3.5°$. The accessible energy range spans from 50-60 GeV (trigger threshold at low zenith angle) up to tens of TeV. The telescope angular resolution (sigma of the Gaussian fit to the point spread function, PSF, σ_{psf}) is about $0.09°$.

Cas A observations were performed between June 2006 and January 2007 for a total observation time of 47 hours after quality cuts, namely, after rejecting runs with detector problems or adverse atmospheric conditions. The zenith angle ranged from $29°$ to $45°$ and averaged $35°$. The observation technique applied was the so-called wobble mode, see Daum et al. (1997) in which the telescope pointed alternatively for 20 minutes to two opposite sky positions at $0.4°$ off the source. Most of the data were taken under moderate moonlight illumination (86% of the scheduled observation time). Depending on the different moonlight levels, the resulting PMT anode currents ranged between 1 μA and 6 μA, as compared to a typical anode current of 1 μA for dark night observations. Correspondingly, the trigger discriminator threshold (DT) was varied between 15 and 30 arbitrary units (a.u.) to keep a low rate of accidental events. The mean trigger discriminator threshold during the observations was 19 a.u, which corresponds to 13.3 photoelectrons (PE). Briefly, the impact of the rise of DT can be summarized by a decrease on the relative γ-ray efficiency from 1 (dark observations) to 0.84 while the relative sensitivity[1] worsens from 2.5 to 2.7% with respect to the Crab flux. Although this effect is important for images containing a low number of PE's (low size), the energy threshold rise (~ 5 GeV) is negligible compared to the rise due to the medium to high zenith angle. Hence, the moderate moonlight illumination did not substantially reduce the telescope performance. More details on the Moon data analysis are discussed by Albert et al. (2007a). Dark and Moon data were analyzed together using the standard analysis and calibration programs for the MAGIC collaboration, e.g. Gaug et al. (2005). The images were cleaned using absolute tail and boundary cuts of 10 and 5 PE, respectively. For the γ/hadron shower separation, the shower images were parameterized using the Hillas parameters, see Hillas et al. (1985). These variables were combined for γ/hadron separation by means of a Random Forest classification algorithm, see Bock et al. (2005), trained with MC simulated γ-ray events and data from galactic areas near the source under study but containing no γ-ray sources. The Random Forest method calculates for every event a parameter dubbed HADRONNESS (H), which parameterizes the purity of

---

^{1} *Minimal flux detectable with 5σ significance in 50 hours of observations.*
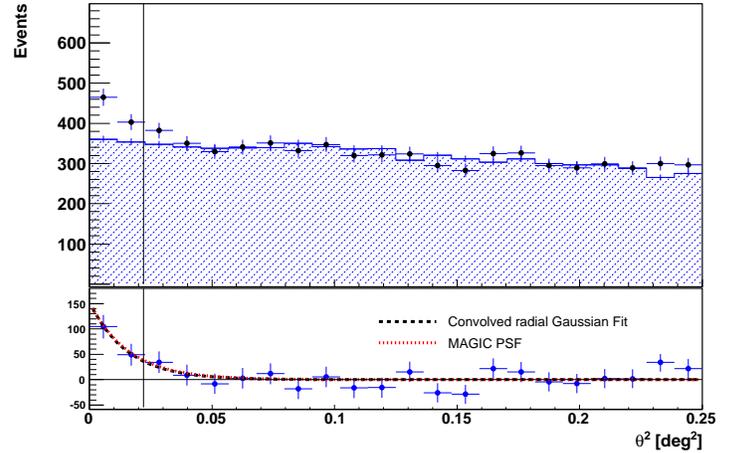

Fig. 1: The upper panel shows the distributions of θ^2 (measured in degree^2) in the direction of the source (black dots) and anti-sources (blue shaded histogram). A lower SIZE cut of 400 PE was applied. The lower panel shows the θ^2 distribution after background subtraction. The vertical line shows the optimum angular cut. The red function corresponds to the telescope PSF and is derived from Crab nebula data taken in the same observational conditions as those for Cas A. The black distribution is the result of a Gaussian fit to the excess distribution.

hadron-initiated images in the multi-dimensional space defined by the Hillas variables.

The θ^2 distribution is computed for the source position, where θ is the angular distance between the source position in the sky and the reconstructed origin position of the shower. The reconstruction of individual γ-ray arrival directions makes use of the so-called DISP method (Domingo-Santamaria et al. (2005)). The expected number of background events are calculated using five regions symmetrically distributed for each wobble position with respect to the center of the camera and refered to as anti-sources.

The optimum H and the angular cuts were derived using dark night Crab data of the same epoch and in the same observation conditions (zenith range, astronomical nights). The use of a dark night data sample in optimizing the telescope sensitivity is justified by the results in Albert et al. (2007a). For the spectral analysis, the energy of each individual γ-ray candidate was also estimated using the Random Forest technique. The average energy resolution for the analyzed energy range was 20%.

3. Source detection, extension and energy spectrum

The so-called θ^2 distributions for the source and anti-source positions are shown in Figure 1 for a lower SIZE cut of 400 PE, which optimizes the MAGIC signal to noise ratio. The black points correspond to the source position whereas the blue-shaded histogram corresponds to the anti-sources. The subtraction of the two histograms shows the excess in the direction of Cas A. An excess of N_{excess}=157 with a significance of 5.2 σ (using the likelihood method of Li & Ma (1983)) is detected within the region $0.13°$ centered at the HEGRA position.

Figure 2 shows the excess map of γ-ray candidates with images larger than 400 PE. The map has been smeared with a Gaussian of σ=$0.07°$. The source position has been determined by ways of a fit of the non-smeared sky map to a bidimensional
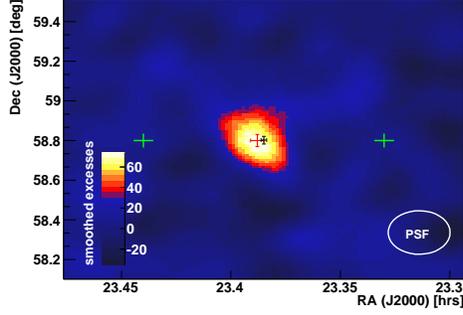
Fig. 2: Sky map around the position of Cas A. A lower cut in SIZE of 400 PE was applied. The green crosses mark the 2 wobble positions. The red cross indicates the MAGIC best fit position. The black cross marks the HEGRA source position, which is within 1 standard deviation from the MAGIC one. The bars of the crosses for both the MAGIC and HEGRA marks correspond to 1 sigma statistical errors.
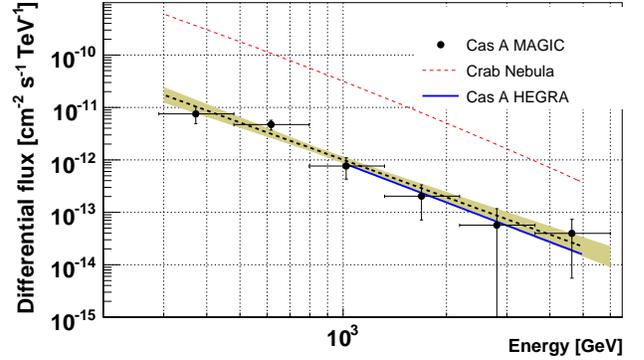

Fig. 3: Cas A spectrum above 250 GeV. The blue line represents the earlier measurement by HEGRA. The red line represents the Crab nebula spectrum. The shaded area is the 1σ statistical error of the fit.

Gaussian function. The best fit position coordinates are RA = $23.386 \pm 0.003_{stat} \pm 0.001_{sys}$ h and DEC = $58.81 \pm 0.03_{stat} \pm 0.02^{\circ}_{sys}$ (for more details on the systematic uncertainties in the source position determination, see Bretz et al. (2005)).

In X-rays and radio-frequencies Cas A has an angular diameter of 0.08°, which is just on the limit of the MAGIC angular resolution. The MAGIC system PSF is derived from MC simulation for a point source, and is found to be σ_{psf}=0.090±0.002° (shown in Figure 2). This value was validated with Mkn 421 and Crab Nebula data (see Albert et al. (2007b)). To further constrain the extension of the source we fit the excess with a Gaussian function convolved with the PSF (F=$A \cdot exp(-0.5\,\theta^2/(\sigma^2_{src} + \sigma^2_{psf}))$). We obtain a value of σ_{src} which is compatible with zero within the fit error. Figure 1 shows the telescope PSF and the result of the Gaussian fit (dotted blue curve).

Figure 3 shows the reconstructed spectrum above 250 GeV. The spectrum is consistent with a power law (dN/dE $\propto$ E$^{-\Gamma}$). The differential flux at 1 TeV is $(1.0 \pm 0.1_{stat} \pm 0.3_{sys}) \times 10^{-12}$ TeV^{-1}cm^{-1}s^{-1} with a photon index of Γ=2.4±0.2$_{stat}$±0.2$_{sys}$.The systematic error is estimated to be 35% in the flux level determination and 0.2 in the spectral index (see Albert et al. (2006)). The measured spectrum was unfolded using the Gauss-Newton method, see Schmelling (1994). The χ^2/d.o.f of the fit is 2.83/3. The 1 σ error limit on the flux fitted is also added as a grey band. The Cas A flux corresponds to an integral flux above 1 TeV of 3% of the Crab nebula flux above the same threshold (in red dashed line in figure 3, see Albert et al. (2007b)). The Cas A spectrum measured by HEGRA is also shown as a blue solid line. The spectrum measured about 8 years later by MAGIC is consistent with that measured by HEGRA for the energies above 1 TeV, i.e, where they overlap.

4. Discussion

The VHE MAGIC 47-hour observation of Cas A confirms the source detection by HEGRA after a multi-year integration of 232 hours and at the same time significantly extends the energy spectrum down to about 250 GeV. Cas A is detected with more than 5 σ at a flux level compatible with the HEGRA measurement for those energies explored in common. The diferential flux at 1 TeV measured by MAGIC is $1.0 \pm 0.1_{stat} \times 10^{-12} TeV^{-1}cm^{-1}s^{-1}$ to be compared with the one measured by HEGRA, $0.9 \pm 0.2_{stat} \times 10^{-12} TeV^{-1}cm^{-1}s^{-1}$. The agreement be-

tween the two measures is excellent not only in the determination of the flux level but also in the spectral index measured. Although the errors in the spectral index are large, there is no evidence for a high energy cutoff, nor for a deviation from a power law at lower energies. The detection of very high energy γ-rays from Cas A provides evidence of the acceleration of multi-TeV particles in SNR shocks and their visibility in gamma-rays Drury et al. (1994).

Significant efforts have been made for the theoretical modeling of Cas A's multi-frequency emission, including that at the highest energies. The effect of an energy-dependent propagation of relativistic electrons in a spatially inhomogeneous medium has been used in order to interpret the radio emission from the region and define its electron content (Atoyan et al. (2000a)). The variations in brightness in the radio band is so complex that a multi-zone model was used: distinguishing between compact, bright spectrum radio knots and the bright fragmented radio ring on one hand, and a diffuse plateau on the other. A three-zone model with a magnetic field decreasing from its highest value in the compact zones putatively related with acceleration sites, to a lower value in regions surrounding the shell, to yet a lower value in the neighborhood has been found to reproduce the radio data, with a magnetic field around and below 1 mG. The fluxes at TeV energies, due to Bremsstrahlung and inverse Compton radiation of the same relativistic electrons have also been computed (Atoyan et al. (2000b)) and, albeit the parameters allow a large range of possible fluxes, the overall shape of the spectrum remains similar, showing a steep cutoff for multi-TeV energies (see, e.g., Figure 7 of Atoyan et al. (2000b)). This cutoff is not seen in HEGRA and/or MAGIC data, disfavoring a leptonic origin of the radiation. Vink and Laming (2003) also studied multi-zone models for Cas A, assuming no difference between zones other than in their magnetic field. They found that an IC origin of high energy fluxes would be possible but only for low values (within the range allowed to be consistent with radio and X-ray observations, see e.g., Vink and Laming 2003, Hwang et al. 2004) of the magnetic field and high, far-infrared photon density. The generally high values of the magnetic field necessary to explain the multi-frequency observations makes it likely that TeV emission from Cas A is then dominated by pion decay (Atoyan et al. 2000b, Vink and Laming 2003).

Berezhko et al. (2003) applied a non-linear kinetic model of cosmic-ray acceleration to describe Cas A, ignoring the role of any small scale inhomogeneities for the production of the very high energy particles and considering the whole SNR blast wave
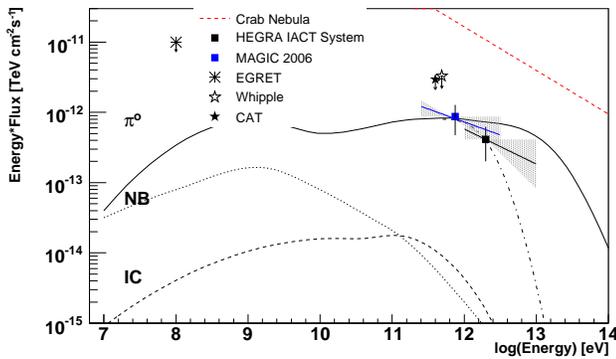
Fig. 4: Spectra of Cas A as measured by MAGIC. The shaded area around the 0.65 TeV detection shows the 1σ statistical error range under the assumption of a $E^{-\alpha}$ power law spectrum. The upper limits given by Whipple, EGRET and CAT are also indicated, as well as the HEGRA detection. The MAGIC and HEGRA spectra are shown in the context of the model by Berezhko et al. (2003). Both hadronic (π^o with and without an energy cutoff) and leptonic (NB and IC) γ-ray emission are shown. The normalization of the pion decay spectrum can be taken as a free parameter.

as the main relativistic particle generator. Figure 4 represents the expected integral γ-ray flux components from non-thermal Bremstrahlung NB, IC scattering on the background radiation field (cosmic microwave + optical/infrared), and hadronic collisions of CR protons with gas nuclei, respectively, for this model. The pion-decay γ-ray flux presented in Figure 4 –with and without an exponential cutoff at 4 TeV– was calculated with a renormalization factor of 1/6 (i.e. this factor takes into account that not all the SNR shock efficiently injects and accelerates cosmic rays). This emphasizes that the normalization of nucleonic predictions of γ-rays is to be considered a free parameter, within certain reasonable boundaries. The predicted slope for the dominating nucleonic-produced γ-rays (that dominates, even when all possible uncertainties leading to an increase of the leptonic emission are included) is hard in the range of interest, as shown in Figure 4, perhaps too hard already to provide a good fit to the new MAGIC data at low energies. Higher and lower energy measurements, and a better signal to noise ratio for the spectrum determination of such a weak source, are still needed for a definite answer.

References

Aharonian, F. et al. 2001, A&A 112, 307.

Albert, J. et al., (MAGIC Collaboration), "Very high energy gamma-ray observations during moonlight and twilight with the MAGIC telescope", submitted to ApJ, astro-ph/0702475, 2007.

Albert, J. et al., (MAGIC Collaboration), "VHE Gamma-Ray Observation of the Crab Nebula and Pulsar with MAGIC" submitted to ApJ, astro-ph/0705.3244, 2007.

Albert, J. et al., (MAGIC Collaboration), 2006, ApJ 638, L101.

Allen, G.E., Gotthelf, E.V. et al., 1997, ApJ 487, L97.

Atoyan, A.M., Tuffs, R.J., & Völk, H.J., 2000a, A&A 354, 915.

Atoyan, A.M., Tuffs, R.J., & Völk, H.J., 2000b, A&A 355, 211.

Bell, A.R., Gull, S.F. & Kenderline, S., 1975, Nature 257, 463.

Berezhko, E.G, Piùhlhofer & Völk, H.J. 2003, A&A 400, 971.

Bretz, T. et al., (MAGIC Collaboration) 2003, Proc. of 28th ICRC (Tsukuba), 2947.

Bock, R. K. et al. 2005, Nucl. Instrum. Meth. A516, 188.

Cortina, J. et al., (MAGIC Collaboration), AIP Conf. Proc. 2005 745, 730.

Daum, A. et al., 1997, Astrop. Physics 8, 1.

Domingo-Santamaria, E. et al., 2005, Proc. of 29th ICRC (Pune) 5, 363.

Drury L.O'C. et al., 1994 , A&A 287, 959.

Esposito, J.A. et al., 1996, ApJ, 461, 820.

Favata, F., Vink, J., Fiume, D.D., et al., 1997, A&A 324, L49.

Fesen, R.A. & Becker, R.H., 1991, ApJ, 371, 621.

Gaug, M. et al., 2005, Proc. 29th ICRC (Pune) 5, 375.

Goret, P., Gouiffes, C., Nuss, E. & Ellison, D.C., 1999, in Proc. of the 26th ICRC, ed. D. Kieda, M. Salamon & B. Dingus (Salt Lake City), vol. 3, 496.

Hillas, A.M., 1985, Proc. of 19th ICRC, La Joya 3, 445.

Hughes, J.P., Rakowski, C.E., Burrows, D.N. & Slane, P.O., 2000, ApJ 528, L109.

Hwang, U. et al., 2004, ApJ Letters 615, 117.

Iyudin, A.F., Diehl, R., Lichti, G.G., et al. 1997, in 2nd INTEGRAL Workshop The Transparent Universe, St. Malo, France (ESA Publications Division, ESTEC, Noordwijk, The Netherlands), 37.

Lessard, R.W., Bond, I.H., Boyle, P.J., et al. 1999, in Proc. of the 26th ICRC, ed. D. Kieda, M. Salamon & B. Dingus (Salt Lake City), vol. 3, 488.

Li, T. & Ma, Y., 1983, ApJ 272, 317.

Reed, J.E., Hester, J.J, Fabian, A.C. & Winkler, P.F., 1995, ApJ 440, 706.

Schmelling, M., 1994, NIM A, 340, 400.

Tuffs, R.J., 1986, MNRAS 219, 13.

Vink, J. & Laming, J. M. 2003, ApJ 584, 758.

Völk, H. J., 1997, in Towards a Major Atmospheric Cherenkov DetectorV, 87, Space Research Unit, O. C. de Jagger Editor.

Young, P.A et al., 2006, ApJ 640, 891

[1] Universität Würzburg, D-97074 Würzburg, Germany

[2] Institut de Física d'Altes Energies, Edifici Cn., E-08193 Bellaterra (Barcelona), Spain

[3] ETH Zurich, CH-8093 Switzerland

[4] Universidad Complutense, E-28040 Madrid, Spain

[5] Universitat Autònoma de Barcelona, E-08193 Bellaterra, Spain

[6] Max-Planck-Institut für Physik, D-80805 München, Germany

[7] Università di Padova and INFN, I-35131 Padova, Italy

[8] Universität Dortmund, D-44227 Dortmund, Germany

[9] University of Łódź, PL-90236 Lodz, Poland

[10] Universitat de Barcelona, E-08028 Barcelona, Spain

[11] Yerevan Physics Institute, AM-375036 Yerevan, Armenia

[12] Tuorla Observatory, Turku University, FI-21500 Piikkiö, Finland

[13] Instituto de Astrofisica de Canarias, E-38200, La Laguna, Tenerife, Spain

[14] Università di Udine, and INFN Trieste, I-33100 Udine, Italy

[15] Università di Siena, and INFN Pisa, I-53100 Siena, Italy

[16] University of California, Davis, CA-95616-8677, USA

[17] Humboldt-Universität zu Berlin, D-12489 Berlin, Germany

[18] Institute for Nuclear Research and Nuclear Energy, BG-1784 Sofia, Bulgaria

[19] INAF/Osservatorio Astronomico and INFN Trieste, I-34131 Trieste, Italy

[20] Università di Pisa, and INFN Pisa, I-56126 Pisa, Italy

[21] ICREA and Institut de Cienciès de l'Espai (IEEC-CSIC), E-08193 Bellaterra, Spain